



**HAL**  
open science

## Differences in local population history at the finest level: the case of the Estonian population

Vasili Pankratov, Francesco Montinaro, Alena Kushniarevich, Georgi Hudjashov, Flora Jay, Lauri Saag, Rodrigo Flores, Davide Marnetto, Marten Seppel, Mart Kals, et al.

### ► To cite this version:

Vasili Pankratov, Francesco Montinaro, Alena Kushniarevich, Georgi Hudjashov, Flora Jay, et al.. Differences in local population history at the finest level: the case of the Estonian population. European Journal of Human Genetics, 2020, 10.1038/s41431-020-0699-4 . hal-02942330

**HAL Id: hal-02942330**

**<https://hal.science/hal-02942330>**

Submitted on 25 Nov 2020

**HAL** is a multi-disciplinary open access archive for the deposit and dissemination of scientific research documents, whether they are published or not. The documents may come from teaching and research institutions in France or abroad, or from public or private research centers.

L'archive ouverte pluridisciplinaire **HAL**, est destinée au dépôt et à la diffusion de documents scientifiques de niveau recherche, publiés ou non, émanant des établissements d'enseignement et de recherche français ou étrangers, des laboratoires publics ou privés.

**1Title:** Differences in local population history at the finest level: the case of the Estonian  
2population

**3Running title:** Genetic structure of Estonia

4*Vasili Pankratov<sup>a,\*</sup>, Francesco Montinaro<sup>a</sup>, Alena Kushniarevich<sup>a</sup>, Georgi Hudjashov<sup>a,b</sup>, Flora*  
5*Jay<sup>c</sup>, Lauri Saag<sup>a</sup>, Rodrigo Flores<sup>a</sup>, Davide Marnetto<sup>a</sup>, Marten Seppel<sup>d</sup>, Mart Kals<sup>a</sup>, Urmo*  
6*Võsa<sup>a</sup>, Cristian Taccioli<sup>e</sup>, Märt Möls<sup>f</sup>, Lili Milani<sup>a</sup>, Anto Aasa<sup>g</sup>, Daniel John Lawson<sup>h</sup>, Tõnu*  
7*Esko<sup>a</sup>, Reedik Mägi<sup>a</sup>, Luca Paganì<sup>a,e,1</sup>, Andres Metspalu<sup>a,1</sup>, Mait Metspalu<sup>a,1</sup>*

8<sup>a</sup>Institute of Genomics, University of Tartu, Tartu, 51010, Estonia;

9<sup>b</sup>Statistics and Bioinformatics Group, School of Fundamental Sciences, Massey University,  
10Palmerston North 4474, New Zealand;

11<sup>c</sup>Laboratoire de Recherche en Informatique, CNRS UMR 8623, Université Paris-Sud,  
12Université Paris-Saclay, Orsay 91405, France

13<sup>d</sup>Institute of History and Archaeology, University of Tartu, Tartu 51005, Estonia;

14<sup>e</sup> Department of Biology, University of Padova, Padova 35131, Italy;

15<sup>f</sup>Institute of Mathematical Statistics, University of Tartu, Tartu 50409, Estonia;

16<sup>g</sup>Institute of Geography University of Tartu, Tartu 51003, Estonia;

17<sup>h</sup>Medical Research Council Integrative Epidemiology Unit, Department of Population Health  
18Sciences, Bristol Medical School, University of Bristol, Bristol BS8 2BN, United Kingdom;

19\*Corresponding author [vasilipankratov@gmail.com](mailto:vasilipankratov@gmail.com)

20<sup>1</sup>Contributed equally

## 21Abstract

22Several recent studies detected fine-scale genetic structure in human populations. Hence,  
23groups conventionally treated as single populations harbour significant variation in terms of  
24allele frequencies and patterns of haplotype sharing. It has been shown that these findings  
25should be considered when performing studies of genetic associations and natural selection,  
26especially when dealing with polygenic phenotypes. However, there is little understanding of  
27the practical effects of such genetic structure on demography reconstructions and selection  
28scans when focusing on recent population history. Here we tested the impact of population  
29structure on such inferences using high-coverage (~30X) genome sequences of 2,305  
30Estonians. We show that different regions of Estonia differ in both effective population size  
31dynamics and signatures of natural selection. By analyzing identity-by-descent segments we  
32also reveal that some Estonian regions exhibit evidence of a bottleneck 10-15 generations  
33ago reflecting sequential episodes of wars, plague, and famine, although this signal is  
34virtually undetected when treating Estonia as a single population. Besides that, we provide a  
35framework for relating effective population size estimated from genetic data to actual census  
36size and validate it on the Estonian population. Our results suggest that the history of human  
37populations within the last few millennia can be highly region-specific and cannot be properly  
38studied without taking local genetic structure into account. Our approach to estimating the  
39census population size may be widely used both to cross-check estimates based on  
40historical sources as well as to get insight into times and/or regions with no other information  
41available.

42

### 43Main text

44As more and more datasets including genetic data from hundreds and thousands of  
45individuals become available it becomes apparent that most if not all human populations  
46exhibit at least some degree of geography-driven genetic structure even at small scales (for  
47some examples see<sup>1-5</sup>). Many recent publications have shown the confounding effect of such  
48population structure on studies of genetic associations and natural selection signals, mainly  
49in the case of polygenic phenotypes<sup>6-9</sup>. Here we study the fine-scale genetic structure of the  
50Estonian population and the local differences in recent demographic history and action of  
51natural selection between genetically defined Estonian subgroups to gain a deeper  
52understanding of the forces shaping this population structure and the consequences it has  
53for population genetics analyses. In doing so we make use of high-coverage whole genome  
54sequences from more than 2300 Estonian individuals generated within a different study<sup>10</sup>.

55Our exploratory principal component analysis (PCA) (Figure 1) shows the presence of  
56genetic structure within Estonia with the main differentiation between South-East and North-  
57East of the country in agreement with previous studies<sup>2,11,12</sup>. To zoom-in into the fine-scale  
58structure in Estonia, we used total genetic length of shared IBD segments detected with  
59*IBDseq*<sup>13</sup> as input for the fineSTRUCTURE<sup>14</sup> clustering algorithm (Methods). We applied this  
60approach to a subset of 468 individuals sampled in rural areas at the age of 50 or more, as  
61this cohort is expected to be the least affected by recent migrations (Figure 2, S11:2.3). We  
62refer to this subset as “R50+” throughout the text (Methods).

63IBD-based analysis (Figure 2) reinforces previous observations<sup>2,11,12</sup>, including the strong  
64differentiation between South-East and the rest of Estonia, and provides a deeper insight  
65into Estonian genetic structure, showing that most of the revealed clusters are highly  
66geographically localized. The sharing matrix provides additional details. First, off-diagonal  
67sharing also reflects geography with clusters from the same area tending to have higher  
68inter-cluster sharing. Second, intra-cluster sharing substantially varies among clusters,

69implying differences in effective population size ( $N_e$ ), which is also supported by the results  
70of homozygosity-by-descent analysis (Figure 3).

71In order to understand how gene flow barriers and/or differences in local population density  
72shaped the IBD-sharing pattern in the R50+ dataset, we inferred migration surfaces using  
73MAPS<sup>15</sup>. We used two windows of IBD segments length (in centimorgans, cM), 2-6 cM and  
74more than 6 cM, which under a simplistic model of infinite population size have mean  
75segment ages of 50 and 12.5 generations respectively<sup>15</sup>. Results for the two length bins  
76generally agree with each other, suggesting higher levels of gene flow in the North along  
77with a barrier separating South-East Estonia (SI1:2.4). A second barrier, separating the  
78islands, especially Hiiumaa, from the mainland is also evident. This observation suggests  
79that the population ancestral to modern South-East Estonians was partially isolated from the  
80rest of the country at least since 50 generations ago. Interestingly, this genetic differentiation  
81is consistent with linguistic data suggesting that the deepest split within the Finnic languages  
82separates Southern Estonian from the other branches of the phylum that includes Northern  
83Estonian<sup>16</sup>.

84As local differences in admixture with external populations may have played a role in  
85creating the observed genetic structure within Estonia we looked at patterns of haplotype  
86sharing between R50+ Estonians and different non-Estonian populations (Table SI2:3.1-I).  
87Here we used a conventional CHROMOPAINTER/fineSTRUCTURE/GLOBETROTTER  
88(CP/FS/GT) approach<sup>17</sup> (Methods). Figure 4 shows the results of non-negative least squares  
89(NNLS)<sup>1</sup>, modelling each individual from the R50+ dataset as a result of admixture between  
90non-Estonian groups revealed by CP/FS (Figure 4, SI1:3.1, Table SI2-3.1-IV).

91Admixture signals in Figure 4 show clear geographic patterns that match known historical  
92evidence of external migration to Estonia, including Swedish settlements on the western  
93coast and islands in 14-15th centuries and Finnish immigration to North-East Estonia in the  
9417th century<sup>18</sup>. Comparing NNLS results between clusters from Figure 2 we found that some  
95of them, such as NE\_1 and NE\_2, stand out in terms of sharing with external groups but  
96most of the clusters have overlapping distributions of NNLS scores (SI1:3.1). A similar

97 pattern is observed in IBD-sharing patterns (SI1:3.2). These results suggest that admixture  
98 with non-Estonian groups can only partially explain the fine genetic structure observed in  
99 Figure 2.

100 We show that, despite the small territory it occupies, the Estonian population exhibits a  
101 readily detectable genetic structure, reflected in patterns of IBD segments sharing (Figure 2)  
102 and allele frequencies (Figure 1, Table SI2-2.3-III, Table SI2-2.3-IV). Next, we sought to  
103 explore whether this differentiation has any effect on the reconstruction of demographic  
104 processes, namely whether there are region-specific differences in effective population size  
105 dynamics and action of natural selection. We hence applied *IBDNe*, which estimates  
106 effective population size ( $N_e$ ) in past generations<sup>19</sup>, and SDS (Singleton Density Score), a  
107 tool for detecting signatures of natural selection<sup>20</sup>, as both methods give insight into very  
108 recent time periods, when regional differences in population history may be anticipated. For  
109 both analyses, we used the entire dataset of 2,305 samples, for which clusters were inferred  
110 using the same approach as for the R50+ subset (Figure 5).

111 We ran *IBDNe*<sup>19</sup> on the four most distinct clusters from Figure 5, representing four regions of  
112 Estonia: North-West, North-East, South-West and South-East and observed rather distinct  
113  $N_e$  trajectories (Figure 6a, SI1:4.2). In particular, all clusters (except for eSE\_5) show  
114 evidence of an effective population size decline between 10 and 20 generations ago, which  
115 is not detected when the entire dataset is analyzed (Figure 6a). Overall, these results  
116 suggest that population dynamics are region-specific and hence population-wide result may  
117 depend on the sampling scheme. For a deeper understanding of this phenomenon and the  
118 effects of other factors on *IBDNe* results, we applied *IBDNe* to genetic data, simulated under  
119 various demographic scenarios (SI1:4.1). Furthermore, the same approach has been applied  
120 to genotype data from the UK population, where regional differences in  $N_e$  dynamics are  
121 observed as well (SI1:4.3).

122 Based on our simulations and MAPS results, we propose that most of the differences in  $N_e$   
123 dynamics between Estonian subpopulations may be attributed to different patterns of gene  
124 flow and external admixture. South-West and North-West Estonia are characterized by an

125 overall high level of gene flow (SI1:2.4), leading to similar  $N_e$  trajectories that deviate only  
126 during the last 20 generations (Figure 6, SI1:4.2) reflecting very recent differences in  
127 population size dynamics and/or migration. This also brings about the idea that the strong  
128 bottleneck in South-West could contribute to the observed population structure, in particular  
129 leading to differentiation of South-West and its subgroups. On the other hand, South-East  
130 Estonia has the most distinct  $N_e$  trajectory according to Figure 6a, having a substantially  
131 lower long-term  $N_e$  compared to other regions. Together with MAPS results (SI1:2.4) this  
132 might suggest a recent expansion of a previously small-size eSE\_5-like population and its  
133 admixture with other local subpopulations occupying South-East Estonia thus contributing to  
134 other eSE groups. This, in turn, results in a rather recent increase in relative proportion of  
135 individuals with eSE\_5-like ancestry in the entire Estonian population affecting the  $N_e$   
136 reconstructions for the entire dataset (SI1:4.2).

137 Given our understanding of confounders of the observed regional  $N_e$  patterns, we exploited  
138 the fine-grained temporal resolution enabled by *IBDNe* to infer changes in actual census  
139 sizes ( $N_c$ ) of the ancestors of contemporary Estonians, adapting previous theoretical work<sup>21</sup>  
140 to empirical case of human populations (Methods). We applied equation [3] (Methods) to the  
141 Estonian-wide  $N_e$  trajectory inferred using the Est1527 subset, which excludes clusters that  
142 can be considered as outliers in terms of external admixture and/or  $N_e$  trajectory (SI1:4.4).  
143 We then compared the inferred  $N_c$  with available historical estimates (Figure 6b) showing a  
144 remarkable match between the two with the exception of the last three generations, for  
145 which *IBDNe* estimates are extrapolated from preceding time points<sup>19</sup>. This match may be  
146 attributed to i) our success in adequately controlling for events of recent gene flow and  
147 population structure; ii) the relatively recent time intervals considered, which limits the range  
148 of spatial interaction among the ancestors of contemporary Estonians. However, note that  
149 the pronounced fluctuations in  $N_c$  reported by historians between 1500 and 1700 are only  
150 very roughly approximated by the  $N_e$ -derived curve which, as expected<sup>22</sup>, provides only  
151 relatively long-term harmonic average of  $N_e$ . Nevertheless, we suggest that after controlling  
152 for confounders such as population structure and admixture and keeping in mind all the

153assumptions implied by the biological notion of  $N_e$ , our approach could be used to convert  
154 $N_e$  to human  $N_c$  at any time interval for which historical records are missing, including the  
155ones provided by PSMC<sup>23</sup>, which are beyond the scope of the current paper.

156We then questioned whether natural selection could have also acted differently within the  
157Estonian population. In doing so, we applied singleton density score (SDS)<sup>20</sup> to the entire  
158dataset of 2,305 samples as well as to two regional subsets, South-East Estonia (SE,  
159consisting of 1,029 samples belonging to clusters eSE\_1 - eSE\_5 in Figure 7) and the  
160remaining 1,276 samples from the rest of the country (nonSE) (Methods, SI1:5.1).

161First, we inspected the genome-wide distribution of positive SDS scores in the three  
162datasets (Figure 7) for any evidence of recent selection acting at individual loci.

163Unlike other studies that used SDS<sup>20,24</sup> we don't observe any hits with very low p-value  
164(possible reasons are discussed in SI1:5.3). However, we see that the distribution of SDS  
165scores differs between the three datasets (Figure 7, Table SI2-5.3-I). Whereas one genome-  
166wide significant hit (rs75386033 and rs79907158 on chromosome 6) is detected in the SE,  
167nonSE and the entire dataset had many more hits with p-values in the range between  $5 \times 10^{-8}$   
168and  $1 \times 10^{-5}$  (Figure 7, SI1:5.3, SI1:5.4, Table SI2-5.3-I). Whereas most of the top SDS signals  
169do not overlap between the three datasets analyzed, one region on chromosome 10  
170corresponding to the *WDFY4* gene appears in both SE and nonSE (Figure 7, Table SI2-5.3-  
171I). It has been shown that *WDFY4* is involved in immune response toward viral and tumor  
172antigens<sup>25</sup> as well as in autoimmune diseases<sup>26-28</sup>. Functional annotation of variants with  
173positive SDS scores<sup>29</sup> coupled with enrichment test<sup>30,31</sup> did not reveal any annotation  
174category to be specific for a particular subset studied (SI1:5.3, SI1:5.4, Tables SI2-5.3-IV-V,  
175Tables SI2-5.4-IV-VII). Likewise, alternative enrichment test employing the GWAS catalog  
176showed that similar phenotype categories are present in the three tested datasets (SI1:5.3,  
177SI1:5.4, Table SI2:5.3-III, Tables SI2:5.4-II-III).

178On the other hand, frequency differences of rs75386033 derived allele T (10.3% in SE vs  
1796.1% in nonSE, Weir and Cockerham<sup>32</sup>  $F_{st}=0.0117$  corresponding to the 0.999 percentile of  
180the genome-wide distribution (Figure S5.4-I) together with its low standardized SDS p-value

181form strong evidence for a recent frequency increase of the rs75386033 T allele in South-  
182East Estonia. Both rs75386033 and rs79907158 lie within an intron of the *GRM1* gene,  
183which is characterized by high levels of expression in the brain  
184(<https://www.ncbi.nlm.nih.gov/gene/2911>). These SNPs themselves are not known to be  
185associated with any phenotypes, however, there are some indications that variant rs362870  
186which is in high linkage disequilibrium with rs75386033 and rs79907158, might be a cis-  
187eQTL for the *EPM2A* gene (SI1:5, Table SI2:5-II), suggesting a plausible biological effect  
188behind the frequency change. *EPM2A* gene is associated with Lafora disease which is a  
189form of progressive myoclonus epilepsy<sup>33–35</sup>. This gene codes for a protein called laforin  
190which is involved in regulating glycogen synthesis and potentially prevents glycogen  
191accumulation in neurons<sup>33–35</sup>.

192Given the lack of information on the phenotypic effect of this *GRM1* allele and its modestly  
193strong SDS signal, it is unclear whether the raise in frequency happened due to actual  
194selection or because of random genetic drift especially given the fact that South-East  
195Estonians exhibit signals of long-lasting low  $N_e$  and further differentiation into smaller  
196subclusters (Figures 2 and 6). Nevertheless, differential SDS signals between the entire  
197Estonian dataset and its subsets including *GRM1*, *WDFY4*, suggest that recent selection,  
198restricted to regional subpopulations, may remain undetected if population-wide datasets are  
199treated as a single entity.

200In conclusion, here we describe a dataset of more than 2300 high-coverage Estonian  
201genomes from a population genetics perspective making it one of the smallest populations to  
202date with such high-resolution data available. We show that the Estonian population, despite  
203occupying a small area with no strong geographic barriers, is genetically structured and  
204exhibits rather pronounced interregional differences with respect to recent admixture with  
205neighbouring populations, population dynamics and potential action of natural selection.  
206These observations together with results of other studies suggest that population  
207stratification could be ubiquitous in human populations, and should be taken into account in  
208any large-scale genetic study including reconstructions of recent population history. We also

209show that we are able to accurately link effective population size to actual census size based  
210on some simple assumptions about human population age structure and reproduction  
211patterns. We envisage future studies exploiting this framework to ultimately unlock the  
212potential of genomic data to provide a reliable estimate of past human census size, hence  
213informing other historical sciences such as the study of cultural evolution, history and  
214archaeology.

## 215METHODS

### 216*Data reporting*

217No statistical methods were used to predetermine sample size. The experiments were not  
218randomized and the investigators were not blinded to allocation during experiments and  
219outcome assessment.

### 220*Whole Genome Sequencing data*

221We used whole genome sequences of the Estonian Biobank participants reported in Kals et  
222al.<sup>10</sup>. We applied exactly the same criteria for filtering individuals (sequencing quality control  
223filters, match between WGS and chip genotype, total number of SNVs, self-reported  
224Estonian ethnicity etc., see Kals et al.<sup>10</sup> for details) except for relatedness and singleton  
225count (see below). For manipulations with vcf files bcftools-1.8<sup>36</sup> was used unless specified  
226otherwise. Additionally to sample filtering applied by Kals et al.<sup>10</sup>, we removed seven  
227samples with missing call over 3% as well as related individuals. To do so we used PLINK-  
2281.9<sup>37</sup> and KING-2.1.6<sup>38</sup> to estimate relatedness coefficient and removed one individual from  
229each pair with this value equal to 0.0442 or higher, corresponding to third degree relatives.  
230This resulted in a dataset consisting of 2,305 individuals that was used for all downstream  
231analyses.

232For analyses that require phased and/or imputed data (CHROMOPAINTER, SDS) phasing  
233and imputation was done using Eagle v2.3<sup>39</sup> on the dataset consisting of 2,420 samples to

234 benefit from the presence of related individuals and subsequently relevant samples were  
235 extracted.

236 All Estonian Biobank participants have signed a broad informed consent which allows  
237 research in the fields of genetic epidemiology, disease risk factors and population history. All  
238 work at Estonian Biobank is conducted according to the Estonian Human Gene Research  
239 Act. The original study generating the WGS data<sup>10</sup> was approved by the Research Ethics  
240 Committee of the University of Tartu (application number 234/T-12).

#### 241 *The 'Rural above 50 years old' (R50+) panel*

242 As information on parents' and grandparents' birthplace is mostly unavailable for the  
243 samples used here, we subsetted the 2,305 dataset for individuals born in rural areas and  
244 sampled at the age of 50 or older as we expect this cohort to be the least affected by recent  
245 migration and long-distance marriages, hence expecting it to preserve the original genetic  
246 structure. This resulted in a dataset of 474 individuals which we further pruned for PCA  
247 outliers (see below) and samples with more than 10,000 singletons (SI1:1.1-SI1:1.3). Per-  
248 sample number of singletons was estimated using vcfTools-0.1.14<sup>40</sup> on the entire (2,305  
249 samples) non-imputed dataset. We ended up with a panel of 468 individuals, which we call  
250 "R50+".

#### 251 *Non-Estonian samples*

252 To place the Estonian population genetic variation in Eurasian context we compiled two  
253 datasets containing the R50+ Estonian samples each and samples from various populations  
254 predominantly representing West Eurasia. The first dataset used for PCA contained 59  
255 samples from 17 populations sequenced on the Complete Genomics platform, 207 samples  
256 from 8 populations sequenced using Illumina technology and 255 samples from 14  
257 populations genotyped on Illumina arrays (Table SI2-1.2-I). Whole genome sequences were  
258 pruned to keep positions matching those overlapping between genotyping arrays resulting in  
259 approximately 450K SNPs.

260The second dataset used for CHROMOPAINTER/fineSTRUCTURE/GLOBETROTTER  
261except for R50+ Estonians included 425 samples from 27 populations genotyped on Illumina  
262arrays and 175 samples from seven 1000 Genome Project populations (CHB, FIN, GBR,  
263GIH, IBS, TSI, YRI) (Table SI2-3.1-I). Whole genome sequences were pruned to keep  
264positions matching those overlapping between genotyping arrays resulting in approximately  
265500K SNPs.

### 266Principal component analysis

267We ran principal component analysis (PCA) for the entire Estonian dataset in two settings: **a)**  
268with only the 2,305 Estonians and **b)** combining the 2,305 Estonians with 521 non-Estonian  
269samples from 18 European populations (Table SI2-1.2-I). In both cases *smartPCA* from  
270EIGENSOFT-7.2.0<sup>41</sup> was used. In setting **a** we directly ran PCA on the dataset filtering for  
271MAF below 0.01, no-call above 0.03 and positions in LD ( $r^2 > 0.4$  within sliding windows of  
272200 positions). Results obtained in setting **a** were used to identify Estonian samples with  
273extreme position in the PCA plot to be removed from the R50+ panel and from the dataset  
274used for SDS (S1:1.2). In setting **b** we used 255,536 bi-allelic SNPs that overlap between  
275the different datasets and passed LD-pruning ( $r^2 > 0.6$  within sliding windows of 1,000  
276positions), MAF ( $< 0.05$ ) and no-call ( $> 0.05$ ) filters. We first calculated the principal  
277components (PCs) based on all non-Estonian samples and then projected the Estonian  
278individuals onto the first two PCs.

### 279CHROMOPAINTER/fineSTRUCTURE/GLOBETROTTER

280To study genetic similarities between Estonians and other European populations we used  
281the CHROMOPAINTER/fineSTRUCTURE (CP/FS) pipeline<sup>17</sup>. It involves a chromosome  
282“painting” procedure which represents each chromosome of an individual (the recipient) as a  
283mixture of chunks received (copied) from every other individual in the dataset (donor). The  
284number of chunks copied by a recipient from each of the donors makes a “copying vector”  
285which are used in the FS algorithm to group individuals into populations.

286Initial chromosome painting parameters were estimated using 30% of the phased dataset of  
2871068 Estonian and non-Estonian samples (Table S12-3.1-I). FS was run for 15 million MCMC  
288iterations in two parallel runs to assess convergence. The tree-building step was performed  
289using the approach from Leslie et al.<sup>1</sup> and the run with the highest observed posterior  
290likelihood was used to cluster the samples into genetic groups. Inferred FS groups were  
291further manually inspected and clustered into the higher-order FS populations (S1:3.2).  
292These FS groups were used as surrogate populations to infer admixture with  
293GLOBETROTTER and estimate ancestry profile with NNLS.

294Next, GLOBETROTTER (GT)<sup>17</sup> was used to detect signals and dates of admixture for the  
295Estonian groups defined using the approach described above. Unlike many other methods,  
296GT allows the structure of unsampled source populations which were involved in the  
297admixture event(s) to be assessed by modelling them as a mixture of sampled surrogate  
298populations. GT inference was performed using a “regional” approach<sup>17,42</sup>. Estonian clusters  
299were only allowed to copy from external surrogates, but not from other Estonians.  
300CHROMOPAINTER parameters were estimated for each Estonian target group individually  
301and the average over all target populations was used to prepare input copying vectors for  
302GT. Two separate runs, with and without standardization by “NULL” individual, were  
303performed and consistency between runs was checked. To assess whether unbalanced  
304surrogate population sample size could have biased our GT inference, we performed five  
305additional GT runs by down sample both target and surrogate populations to 20 individuals.

306Finally, given complex admixture signal in Estonia, we implemented non-negative least-  
307squares (NNLS) method<sup>1</sup>. This allowed us to assign relative ancestral proportions to each  
308individual in the R50+ panel using the non-Estonian surrogate groups identified by FS as  
309sources. NNLS values for CP/FS Estonian groups were extracted from GT output while for  
310individual samples these were calculated with an in-house R script. Obtained results were  
311then summarized across Estonian parishes as well as across IBD/FS clusters.

312*Detecting segments identical-by-descent (IBD segments)*

313 To detect IBD segments in the Estonian dataset we applied *IBDseq* version r1206 (10) with  
314 default settings (errormax=0.001, errorprop=0.25, r2window=500, r2max=0.15, minalleles=2,  
315 lod=3.0) to the non-phased non-imputed dataset consisting of 2,305 Estonians. Choosing  
316 *IBDseq* over *refined IBD*<sup>43</sup> here is justified by working with samples coming from a relatively  
317 homogeneous population, which makes *IBDseq* frequency model applicable, while *IBDseq*  
318 has the advantage of not requiring phasing as well as having sequencing errors and rare  
319 alleles being explicitly accounted for. As *IBDseq* software reports only physical coordinates  
320 of a segment's start and end we interpolated segments' genetic length in cM using GRCh37  
321 recombination map ([ftp://ftp.ncbi.nlm.nih.gov/hapmap/recombination/2011-01\\_phaseII\\_B37/](ftp://ftp.ncbi.nlm.nih.gov/hapmap/recombination/2011-01_phaseII_B37/))  
322 using R<sup>44</sup>. When working with the R50+ panel corresponding IBD segments were retrieved  
323 from the general output obtained on the 2,305 dataset. Homozygosity-by-descent segments  
324 were also inferred with *IBDseq*.

325 IBD segments between Estonians and non-Estonian individuals were detected by applying  
326 *refined IBD* version 12Jul18.a0b<sup>43</sup> with default parameters except for length (window=40.0,  
327 length=1.0, trim=0.15, lod=3.0) to the same dataset that was used for CP/FS/GT, as in this  
328 case the dataset is highly structured. This was followed by applying the *merge-ibd* utility  
329 version 12Jul18.a0b to merge together segments separated by at most 1 cM long gaps and  
330 no more than 2 positions with genotypes discordant with IBD.

331 Both for *IBDseq* and *refined IBD/ibd-merge* results segments shorter than 2 cM were  
332 discarded, as longer segments are detected with higher reliability.

### 333 MAPS

334 In order to evaluate the extent of gene flow across the whole country together with local  
335 population densities, we estimated migration surfaces using MAPS<sup>15</sup>, which harnesses a  
336 similarity matrix summarizing the total number of IBD segments shared in a given  
337 population. In doing so, we used the IBD segments shared among pairs of individuals  
338 inferred with *IBDseq* as described in the previous section. Subsequently we have classified  
339 the shared genetic fragments as "short" (between 2 and 6 cM) and "long" (more than 6 cM),

340 and performed two independent MAPS runs for each length class to assess convergence.  
341 Estonian territory was modeled as having a total of 200 demes. Each run had 5 million  
342 iterations thinned every 10,000 and preceded by a burn-in of 2 million discarded cycles. The  
343 obtained migration surfaces were subsequently plotted using the plotmaps R package<sup>15</sup>. We  
344 repeated the whole procedure after removing samples belonging to clusters from Figure 2  
345 with mean sharing above 60 cM to assess their effect on MAPS results.

#### 346 *IBD-based fineSTRUCTURE (IBD/FS)*

347 In order to exploit patterns of genetic similarity between samples that arose very recently  
348 and get insight into fine genetic structure of the Estonian population, we used total genetic  
349 length of IBD segments longer than 2 cM as a measure of genetic similarity between pairs of  
350 individuals. We refer to this measure as “IBD-sharing”. Next, to obtain natural genetic  
351 grouping of the samples we used a matrix of IBD-sharing as input for fineSTRUCTURE  
352 v2.0.7<sup>14</sup>. Although our approach is different from the original  
353 CHROMOPAINTER/fineSTRUCTURE method<sup>14</sup>, it is very similar in its idea to the approach  
354 used in <sup>3</sup>, and, put loosely, treats each cM shared between a pair of individuals as a  
355 CHROMOPAINTER chunk copied by the recipient from the donor. The fineSTRUCTURE  
356 algorithm already has an inbuilt method of compensating for the fact that the units used to  
357 measure similarity/relatedness between samples (either chunks in the classical approach or  
358 cM in our approach) don’t represent fully independent pieces of information by transforming  
359 the raw value into an effective one by applying a *c*-factor. The *c*-factor was calculated using  
360 the *fs combine* command with the -C option applied to matrices of IBD-sharing for each  
361 individual chromosome. For more details see Supplementary Information SI1:2.1 and  
362 SI1:2.2. When running fineSTRUCTURE for both R50+ and the entire dataset the first  
363 2,000,000 MCMC iterations were removed as burn-in and subsequently MCMC was run for  
364 additional 2,000,000 MCMC iterations sampling every 10,000th run. When building the tree  
365 we used the approach described in Leslie et al., 2015<sup>1</sup> and corresponding to the “1” value of  
366 the -T option in fineSTRUCTURE v2, which, put informally, maximizes the concordance

367between samples' final cluster assignment and its' assignment in individual MCMC runs. To  
368validate this approach we applied it to the simulated data used in Lawson et al., 2012<sup>14</sup>, and  
369calculated the same measure of correlation between real and inferred cluster assignment of  
370the samples for different number of chromosomal regions used to detect IBD segments  
371(SI1:2.2).

372We applied this approach to the R50+ dataset (468 samples) and the entire dataset (2,305  
373samples). In both cases fineSTRUCTURE was run twice to assess convergence (SI1:2.3,  
374Tables SI2-2.3-I and SI2-2.3-II). In the case of the R50+ dataset to reduce the number of  
375clusters revealed by the fineSTRUCTURE algorithm we have hierarchically joined together  
376clusters with short terminal branches by cutting the tree at such a level so as to avoid having  
377clusters consisting of less than 5 samples. In the case of the entire dataset clusters referred  
378to throughout the text were obtained by cutting the tree at a level chosen after visual  
379inspection (SI1:2.3).

#### 380*Fst calculations*

381Fst between Estonian clusters was calculated using smartpca from the EIGENSOFT  
382package v7.2.0<sup>41</sup> after LD-pruning ( $r^2 > 0.4$ , windows of 1,000 SNPs) and removing sites with  
383MAF < 0.05 and missing rate > 0.1.

384Per-site Weir and Cockerham<sup>32</sup> Fst estimator between SE and nonSE subsets was  
385calculated using vcfTools<sup>40</sup> after filtering sites for LD, MAF and missing rate the same way as  
386described above.

#### 387*Geographic data visualization*

388Geographic coordinates of the corresponding birth town/parish were assigned to each  
389sample with birth place information available (2,168 out of 2,305 samples). For MAPS these  
390coordinates were used directly. When plotting IBD/FS and NNLS results for the R50+ panel,  
391coordinates of the samples were changed manually to avoid over-plotting. When plotting  
392samples from the entire dataset jittering was used for the same purpose. Shp objects used  
393to plot maps of Estonia with parish and county borders were retrieved from the Estonian

394Land Board website (Administrative and settlement units, 2018.11.01,  
395[https://geoportaal.maaamet.ee/eng/Spatial-Data/Administrative-and-Settlement-Division-](https://geoportaal.maaamet.ee/eng/Spatial-Data/Administrative-and-Settlement-Division-396p312.html)  
396p312.html). Geographic data were visualized in R<sup>44</sup> with the aid of the following packages:  
397sp<sup>45,46</sup>, sf<sup>47</sup>, rgdal<sup>48</sup>, rgeos<sup>49</sup> and ggplot2<sup>50</sup>.

#### 398*IBDNe*

399In order to reconstruct recent Ne dynamics we used *IBDNe* version 07May18.6a<sup>19</sup> with  
400default settings (npairs=0, nits=1000, nboots=80, trimcm=0.2). *IBDNe* was applied to sets of  
401no less than 100 individuals. In all cases IBD segments used as input for *IBDNe* were  
402detected with *IBDseq*<sup>13</sup>. Recombination map in PLINK format used to convert physical  
403distances to the genetic ones was taken from  
404[http://bochet.gcc.biostat.washington.edu/beagle/genetic\\_maps/plink.GRCh37.map.zip](http://bochet.gcc.biostat.washington.edu/beagle/genetic_maps/plink.GRCh37.map.zip).

405To get independent evidence of regional differences in Ne dynamics we applied *IBDNe* to  
406samples from the People of the British Isles<sup>1</sup> dataset grouped by the region of origin of  
407individuals' grandparents. The following regions were used: Scotland, Wales and North-East,  
408North-West, South-East and South-West England. For the list of counties comprising these  
409regions see Table S2:4.3-I.

#### 410*Genetic simulations*

411To simulate genetic data under various demographic scenarios to test the behavior of *IBDNe*  
412we used mspms which is an ms-compatible version of msprime<sup>51</sup>. Commands used for  
413simulation are provided in the Supplementary Information S1:4.1.

#### 414*Estimating actual census size based on Ne*

415Several lines of evidence, based both on theoretical reasoning<sup>52</sup> and empirical  
416comparisons<sup>19</sup> suggest that in industrial human societies census size (Nc) is roughly 3 fold  
417the Ne assuming a panmictic and isolated population. However, application of this coefficient  
418is limited to populations with specific reproductive characteristics, for example 1:1 male to  
419female ratio and Poisson distribution of number of offspring among individuals capable of

420reproducing. We therefore adapted a more general approach from<sup>22</sup> which incorporates the  
 421inbreeding coefficient ( $F_{is}$ ), relative fraction of males ( $m$ ) and excess in variance of  
 422reproductive success compared to the Poisson distribution ( $DV$ ):

$$423 \quad N_{b(t)} = \frac{(1+F_{is})}{4} \times \left( \frac{1}{(1-m) \times m} + DV \right) \times N_{e(t)}$$

424 [1]

425Formula [1] yields the  $N_b$ , the number of breeding individuals (individuals capable of  
 426reproducing) at time  $t$  under the assumption of absence of gene flow and population  
 427structure, non-overlapping generations and equal variance of number of offspring between  
 428sexes. It is dependent on parameters such as  $m$ ,  $F_{is}$  and  $DV$  that cannot be reliably  
 429estimated for each time bin. We therefore explored a range of plausible scenarios described  
 430by different values of  $m$ ,  $F_{is}$  and  $DV$  based on the following assumptions: i)  $F_{is}$  calculated on  
 431chromosome 1 for contemporary human populations from the 1000 genomes dataset<sup>53</sup> as  
 432well as for Estonians ranges from  $-0.016$  to  $0.004$  (S1:4.4), leading to the conclusion that for  
 433most human populations the term  $(1+F_{is})$  can be safely approximated to 1; ii)  $m$ , the relative  
 434fraction of reproducing males, must be comprised between 0.1 and 0.9, considering further  
 435polarizations of this parameter as implausible for our species; iii)  $DV$ , the difference between  
 436the expected and the observed variance in number of offspring per adult can be estimated to  
 437range between  $-1$  and 3. The latter estimate was obtained by taking Poisson distributions  
 438constrained between 0 and 10 (considering 10 as the maximum number of surviving children  
 439per adult) with an average between 1 and 5, and by empirically inflating the most extreme  
 440bins (0 or 10 children per adult) 5-fold. Such an exercise yields  $DVs$  ranging between  $-0.2$   
 441and 2.5, which we conservatively rounded to  $-1$  and 3, respectively. This range is also  
 442consistent with data from contemporary Estonians, available from the Estonian Biobank, and  
 443showing a  $DV$  of  $-0.76$  based on 7,863 females born between 1900 and 1955 and in the age  
 444of menopause at the time of enrolment. When plugged together into formula [1], these  
 445estimates yield a minimum of 0.75 (with  $m=0.5$  and  $DV=-1$ ) and a maximum of 3.53 (with  
 446 $m=0.1$  or  $0.9$  and  $DV=3$ ). To provide a single point estimate of  $N_c$  we rewrite formula [1] as

$$447 \quad N_{b(t)} = 1.63 \times N_{e(t)}$$

448[2]

449using a geometric mean between 0.75 and 3.5 and thus making our estimate slightly more  
450than 2-fold away from the provided range boundaries. Note, that although there are  
451indications that in some human populations DV can be higher than  $3^{54}$ , such cases can be  
452considered to be at the very extreme of human reproductive behaviour spectrum as even  
453hypothetical “super-male” populations would have a sex-average DV of 1.8 given  $m$  equals  
454to  $0.5^{55}$ . Hence we suggest our approach to be applicable to many human populations  
455provided that immigration and population structure can be properly accounted for. In  
456addition, the range of DV can be changed to study populations with extreme inequality in  
457reproductive success.

458The value estimated using [2] corresponds to the number of individuals in reproductive age.  
459It can be converted into total census size ( $N_c$ ) of a human population at a given time point by  
460dividing it by the estimated fraction of breeding individuals, which we here assume to be  
461roughly 0.33. This is supported by actual data on the Estonian population from the “Statistics  
462Estonia” database (<http://andmebaas.stat.ee/Index.aspx?lang=en#>) showing that the fraction  
463of people between 20 and 40 years old was between 0.33 to 0.38 during the period between  
4641970 and 2018. Incorporating this idea into [2] results in equation [3].

$$465 \quad N_{c(t)} = 4.89 \times N_{e(t)}$$

466[3]

467which we used to obtain the curve in Figure 6B. Sources of historical estimates of Estonian  
468population size used in that figure are provided in S4.2-II.

469When using  $N_e$  as a proxy for actual population size one should keep in mind the potential  
470effect of gene flow between populations. For example under a stepping stone model with  
471constant population size and migration  $N_e$  estimated using samples from one deme is  
472expected to increase when going back in time as more and more ancestors of sampled  
473individuals would represent other demes<sup>56</sup>. In other words, coalescent-based  $N_e$  estimates

474 reflect the number of ancestors of a sampled population, which may have lived in any  
475 location in space, rather than strictly the number of individuals in a given area at a given time  
476 point.

#### 477 *Singleton density score (SDS) selection scan*

478 As SDS<sup>20</sup> does not handle missing data, imputed genomes of 2,301 unrelated individuals  
479 (four PCA outliers removed) were used. SDS<sup>20</sup> analysis was applied to three datasets  
480 separately, namely, the entire dataset and its two subsets, Estonia SE and Estonia nonSE.  
481 The latter two were defined based on the IBD/FS results (Figure 5): SE (individuals with  
482 South-East Estonian ancestry belonging to clusters eSE\_1-eSE\_5) and nonSE (individuals  
483 coming from the other parts of the country and belonging to other clusters). We did not apply  
484 SDS to finer subclusters of the dataset due to sample size issues. The number of individual  
485 genomes used in the analysis has a direct impact on the number of SNPs analyzed, the  
486 power to detect selection at any given SNP and the length of the terminal branches of the  
487 coalescent tree and hence the timing of the selection events that can be inferred<sup>20</sup>. Since in  
488 this study we are focusing on recent selection signals and differences between  
489 subpopulations that show only limited differentiation, we aimed at using samples of at least  
490 1000 individuals. As the dataset needs to be homogeneous in terms of number of singletons  
491 per individual, this value was calculated with vcfTools 0.1.14<sup>40</sup> independently for each of the  
492 datasets and individuals with extreme values (below 5th or above 95th quantiles) were  
493 removed. Final datasets included 2,076, 927 and 1,132 samples for the entire dataset, SE  
494 and nonSE subsets respectively. Predicted functional effect of the test SNPs was assessed  
495 using Combined Annotation-Dependent Depletion tool (CADD)<sup>29</sup>. In addition, two alternative  
496 enrichment tests were performed to see whether candidate SNPs are enriched in a certain  
497 category of genes<sup>30,31</sup> or in certain GWAS catalogue categories  
498 (<http://www.ebi.ac.uk/gwas/home>;<sup>57</sup>). Candidate SNPs, as well as SNPs in linkage  
499 disequilibrium with those ( $R^2 > 0.5$ ), were checked for known e-QTL effects using the

500eQTLGen Consortium<sup>58</sup> (<http://www.eqtlgen.org/>) database. Details of SNP annotation and  
501enrichment analyses are specified in S1:5.2.

## 502DATA AVAILABILITY

503The sequencing data are available on demand. The procedure of applying for the access to  
504the data can be found under the following link:  
505<https://www.geenivaramu.ee/en/biobank.ee/data-access>.

## 506REFERENCES

- 5071 Leslie S, Winney B, Hellenthal G *et al*. The fine-scale genetic structure of the British  
508 population. *Nature* 2015; **519**: 309–314.
- 5092 Martin AR, Karczewski KJ, Kerminen S *et al*. Haplotype Sharing Provides Insights into  
510 Fine-Scale Population History and Disease in Finland. *Am J Hum Genet* 2018; **102**:  
511 760–775.
- 5123 Bycroft C, Fernandez-Rozadilla C, Ruiz-Ponte C *et al*. Patterns of genetic differentiation  
513 and the footprints of historical migrations in the Iberian Peninsula. *Nat Commun* 2019;  
514 **10**: 551.
- 5154 Raveane A, Aneli S, Montinaro F *et al*. Population structure of modern-day Italians  
516 reveals patterns of ancient and archaic ancestries in Southern Europe. *Sci Adv* 2019; **5**:  
517 eaaw3492.
- 5185 Saint Pierre A, Giemza J, Alves I *et al*. The genetic history of France. *Eur J Hum Genet*  
519 2020; : 1–13.
- 5206 Berg JJ, Harpak A, Sinnott-Armstrong N *et al*. Reduced signal for polygenic adaptation  
521 of height in UK Biobank. *eLife* 2019; **8**: e39725.

- 5227 Sohail M, Vakhrusheva OA, Sul JH *et al.* Negative selection in humans and fruit flies  
523 involves synergistic epistasis. *Science* 2017; **356**: 539–542.
- 5248 Haworth S, Mitchell R, Corbin L *et al.* Apparent latent structure within the UK Biobank  
525 sample has implications for epidemiological analysis. *Nat Commun* 2019; **10**: 333.
- 5269 Kerminen S, Martin AR, Koskela J *et al.* Geographic Variation and Bias in the Polygenic  
527 Scores of Complex Diseases and Traits in Finland. *Am J Hum Genet* 2019; **104**: 1169–  
528 1181.
- 52910 Kals M, Nikopensius T, Läll K *et al.* Advantages of genotype imputation with ethnically  
530 matched reference panel for rare variant association analyses. *bioRxiv* 2019; : 579201.
- 53111 Nelis M, Esko T, Mägi R *et al.* Genetic Structure of Europeans: A View from the North–  
532 East. *PLOS ONE* 2009; **4**: e5472.
- 53312 Haller T, Leitsalu L, Fischer K *et al.* MixFit: Methodology for Computing Ancestry-Related  
534 Genetic Scores at the Individual Level and Its Application to the Estonian and Finnish  
535 Population Studies. *PLoS ONE* 2017; **12**. doi:10.1371/journal.pone.0170325.
- 53613 Browning BL, Browning SR. Detecting Identity by Descent and Estimating Genotype  
537 Error Rates in Sequence Data. *Am J Hum Genet* 2013; **93**: 840–851.
- 53814 Lawson DJ, Hellenthal G, Myers S, Falush D. Inference of Population Structure using  
539 Dense Haplotype Data. *PLoS Genet* 2012; **8**: e1002453.
- 54015 Al-Asadi H, Petkova D, Stephens M, Novembre J. Estimating recent migration and  
541 population-size surfaces. *PLOS Genet* 2019; **15**: e1007908.
- 54216 Kallio P. The Diversification of Proto-Finnic. In: Ahola J, Frog, Tolley C (eds). *Fibula,*  
543 *Fabula, Fact: The Viking Age in Finland*. BoD - Books on Demand, 2018.

- 54417 Hellenthal G, Busby GBJ, Band G *et al.* A genetic atlas of human admixture history.  
545 *Science* 2014; **343**: 747–751.
- 54618 Loit A. Invandringen från Finland till Baltikum under 1600-talet. *Hist Tidskr För Finl* 1982;  
547 : 194–195.
- 54819 Browning SR, Browning BL. Accurate Non-parametric Estimation of Recent Effective  
549 Population Size from Segments of Identity by Descent. *Am J Hum Genet* 2015; **97**: 404–  
550 418.
- 55120 Field Y, Boyle EA, Telis N *et al.* Detection of human adaptation during the past 2000  
552 years. *Science* 2016; **354**: 760–764.
- 55321 Laporte V, Charlesworth B. Effective Population Size and Population Subdivision in  
554 Demographically Structured Populations. *Genetics* 2002; **162**: 501–519.
- 55522 Charlesworth B. Fundamental concepts in genetics: effective population size and  
556 patterns of molecular evolution and variation. *Nat Rev Genet* 2009; **10**: 195–205.
- 55723 Li H, Durbin R. Inference of human population history from individual whole-genome  
558 sequences. *Nature* 2011; **475**: 493–496.
- 55924 Okada Y, Momozawa Y, Sakaue S *et al.* Deep whole-genome sequencing reveals recent  
560 selection signatures linked to evolution and disease risk of Japanese. *Nat Commun*  
561 2018; **9**. doi:10.1038/s41467-018-03274-0.
- 56225 Theisen DJ, Davidson JT, Briseño CG *et al.* WDFY4 is required for cross-presentation in  
563 response to viral and tumor antigens. *Science* 2018; **362**: 694–699.
- 56426 Yuan Q, Li Y, Li J *et al.* WDFY4 Is Involved in Symptoms of Systemic Lupus  
565 Erythematosus by Modulating B Cell Fate via Noncanonical Autophagy. *J Immunol*  
566 *Baltim Md 1950* 2018; **201**: 2570–2578.

- 56727 Zhang Y, Bo L, Zhang H, Zhuang C, Liu R. E26 Transformation-Specific-1 (ETS1) and  
568 WDFY Family Member 4 (WDFY4) Polymorphisms in Chinese Patients with Rheumatoid  
569 Arthritis. *Int J Mol Sci* 2014; **15**: 2712–2721.
- 57028 McIntosh LA, Marion MC, Sudman M *et al*. Genome-Wide Association Meta-Analysis  
571 Reveals Novel Juvenile Idiopathic Arthritis Susceptibility Loci. *Arthritis Rheumatol*  
572 *Hoboken NJ* 2017; **69**: 2222–2232.
- 57329 Kircher M, Witten DM, Jain P, O’Roak BJ, Cooper GM, Shendure J. A general framework  
574 for estimating the relative pathogenicity of human genetic variants. *Nat Genet* 2014; **46**:  
575 310–315.
- 57630 Chen EY, Tan CM, Kou Y *et al*. Enrichr: interactive and collaborative HTML5 gene list  
577 enrichment analysis tool. *BMC Bioinformatics* 2013; **14**: 128.
- 57831 Kuleshov MV, Jones MR, Rouillard AD *et al*. Enrichr: a comprehensive gene set  
579 enrichment analysis web server 2016 update. *Nucleic Acids Res* 2016; **44**: W90-97.
- 58032 Weir B, Clark Cockerham C. Weir BS, Cockerham CC.. Estimating F-Statistics for the  
581 Analysis of Population-Structure. *Evolution* 38: 1358-1370. *Evolution* 1984; **38**: 1358–  
582 1370.
- 58333 Minassian BA, Lee JR, Herbrick JA *et al*. Mutations in a gene encoding a novel protein  
584 tyrosine phosphatase cause progressive myoclonus epilepsy. *Nat Genet* 1998; **20**: 171–  
585 174.
- 58634 Serratosa JM, Gómez-Garre P, Gallardo ME *et al*. A novel protein tyrosine phosphatase  
587 gene is mutated in progressive myoclonus epilepsy of the Lafora type (EPM2). *Hum Mol*  
588 *Genet* 1999; **8**: 345–352.
- 58935 Nitschke F, Ahonen SJ, Nitschke S, Mitra S, Minassian BA. Lafora disease - from  
590 pathogenesis to treatment strategies. *Nat Rev Neurol* 2018; **14**: 606–617.

- 59136 Li H, Handsaker B, Wysoker A *et al*. The Sequence Alignment/Map format and  
592 SAMtools. *Bioinforma Oxf Engl* 2009; **25**: 2078–2079.
- 59337 Purcell S, Neale B, Todd-Brown K *et al*. PLINK: a tool set for whole-genome association  
594 and population-based linkage analyses. *Am J Hum Genet* 2007; **81**: 559–575.
- 59538 Manichaikul A, Mychaleckyj JC, Rich SS, Daly K, Sale M, Chen W-M. Robust  
596 relationship inference in genome-wide association studies. *Bioinformatics* 2010; **26**:  
597 2867–2873.
- 59839 Loh P-R, Palamara PF, Price AL. Fast and accurate long-range phasing in a UK Biobank  
599 cohort. *Nat Genet* 2016; **48**: 811–816.
- 60040 Danecek P, Auton A, Abecasis G *et al*. The variant call format and VCFtools. *Bioinforma*  
601 *Oxf Engl* 2011; **27**: 2156–2158.
- 60241 Patterson N, Price AL, Reich D. Population structure and eigenanalysis. *PLoS Genet*  
603 2006; **2**: e190.
- 60442 Hudjashov G, Karafet TM, Lawson DJ *et al*. Complex Patterns of Admixture across the  
605 Indonesian Archipelago. *Mol Biol Evol* 2017; **34**: 2439–2452.
- 60643 Browning BL, Browning SR. Improving the Accuracy and Efficiency of Identity-by-  
607 Descent Detection in Population Data. *Genetics* 2013; **194**: 459–471.
- 60844 R Core Team. *R: A language and environment for statistical computing*. R Foundation for  
609 Statistical Computing: Vienna, Austria, 2018<https://www.R-project.org/>.
- 61045 Pebesma E, Bivand R. Classes and methods for spatial data in R. *R News* 2005; **5**: 9–  
611 13.

- 61246 Bivand RS, Pebesma E, Gómez-Rubio V. *Applied Spatial Data Analysis with R*. 2nd ed.  
613 Springer-Verlag: New York, 2013<https://www.springer.com/gp/book/9781461476177>  
614 (accessed 18 Jun2019).
- 61547 Pebesma E. Simple Features for R: Standardized Support for Spatial Vector Data. *R J*  
616 2018.<https://journal.r-project.org/archive/2018/RJ-2018-009/>.
- 61748 Bivand R, Keitt T, Rowlingson B *et al.* *rgdal: Bindings for the 'Geospatial' Data*  
618 *Abstraction Library*. 2019<https://CRAN.R-project.org/package=rgdal> (accessed 18  
619 Jun2019).
- 62049 Bivand R, Rundel C, Pebesma E *et al.* *rgeos: Interface to Geometry Engine - Open*  
621 *Source ('GEOS')*. 2019<https://CRAN.R-project.org/package=rgeos> (accessed 18  
622 Jun2019).
- 62350 Wickham H. *ggplot2: Elegant Graphics for Data Analysis*. Springer-Verlag: New York,  
624 2009<https://www.springer.com/gp/book/9780387981413> (accessed 18 Jun2019).
- 62551 Kelleher J, Etheridge AM, McVean G. Efficient Coalescent Simulation and Genealogical  
626 Analysis for Large Sample Sizes. *PLOS Comput Biol* 2016; **12**: e1004842.
- 62752 Felsenstein J. Inbreeding and Variance Effective Numbers in Populations with  
628 Overlapping Generations. *Genetics* 1971; **68**: 581–597.
- 62953 The 1000 Genomes Project Consortium. A global reference for human genetic variation.  
630 *Nature* 2015; **526**: 68–74.
- 63154 Austerlitz F, Heyer E. Social transmission of reproductive behavior increases frequency  
632 of inherited disorders in a young-expanding population. *Proc Natl Acad Sci U S A* 1998;  
633 **95**: 15140–15144.

63455 Heyer E, Chaix R, Pavard S, Austerlitz F. Sex-specific demographic behaviours that  
635 shape human genomic variation. *Mol Ecol* 2012; **21**: 597–612.

63656 Browning SR, Browning BL, Daviglus ML *et al*. Ancestry-specific recent effective  
637 population size in the Americas. *PLoS Genet* 2018; **14**: e1007385.

63857 MacArthur J, Bowler E, Cerezo M *et al*. The new NHGRI-EBI Catalog of published  
639 genome-wide association studies (GWAS Catalog). *Nucleic Acids Res* 2017; **45**: D896–  
640 D901.

64158 Võsa U, Claringbould A, Westra H-J *et al*. Unraveling the polygenic architecture of  
642 complex traits using blood eQTL metaanalysis. *bioRxiv* 2018; : 447367.

#### 643 **Author Contribution**

644VP, LP, AM and MM designed the study. LS, TE, RM, LP and AM conducted sample  
645management and provided access to data. MS provided historical data. VP, FM, AK, GH, FJ,  
646RF, DM, MK, AA, DJL and LP analyzed the data. VP, FM, AK, GH, FJ, LS, RF, DM, MS, UV,  
647MK, CT, MMo, LM, AA, DJL, TE, RM, LP, AM, MM contributed to the interpretation of results.  
648VP, FM, AK, GH, FJ, RF, DM, MS, CT, DJL, LP, MM wrote the manuscript.

#### 649 **Acknowledgements**

650This work was supported by the Estonian Research Council grants PRG243 (GH, RF, LS,  
651LP, MM), PUT1339 (AK), PUTJD817 (MK), MOBTP108 (UV), IUT20-60 (AM, RM), IUT24-6  
652(AM, RM), PUT1660 (TE) and PRG184 (LM); by the European Union through the European  
653Regional Development Fund Projects No. 2014-2020.4.01.16-0030 (FM, MM, VP), No.  
6542014-2020.4.01.15-0012 (AM, RM, TE, LM, GH, LS, MM), No. 2014-2020.4.01.16-0024  
655(DM, LP, VP), No. 2014-2020.4.01.16-0125 (RF), No. 2014-2020.4.01.16-0271 (RF) and  
6562014-2020.4.01.16-0125 (AM, RM, TE, LM); by NIH GIANT (AM, TE); by ERA-CVD grant

657Detectin-HF (AM), by NIH-BMI Grant 2R01DK075787-06A1 (TE), by the Wellcome Trust No.  
658WT104125MA (DJL) as well as by the European Union through Horizon 2020 grant no.  
659810645 (MM) and PRESICE4Q (LM).

660Data analysis was performed on the High-Performance Computing Center of University of  
661Tartu.

662The authors would like to thank the Genome Aggregation Database (gnomAD) and the  
663groups that provided exome and genome variant data to this resource. A full list of  
664contributing groups can be found at <https://gnomad.broadinstitute.org/about>.

665The authors would like to thank Bayazit Yunusbayev for fruitful discussion and valuable  
666advice.

#### 667**Competing interests**

668Authors declare no competing interests.

#### 669**Figures**

670Figure 1. Principal components analysis of 2,305 Estonian samples in the context of West  
671Eurasian populations. Estonian samples were projected onto PC space defined by European  
672samples (Methods, SI1:1.1, SI1:1.2, Table SI2:1.1-I, Table SI2:1.2-I). Outlined labelled dots  
673correspond to medians of European populations or Estonian counties while non-outlined  
674dots represent individual samples. Estonian samples are shown in colour corresponding to  
675the geographic region of origin: NW (North-West) included Harjumaa (Ha), Läänemaa (Lä),  
676Raplamaa (Ra), Järvamaa (Jä), Hiiumaa (Hi) and Saaremaa (Sa) counties; NE (North-East)  
677includes Lääne-Virumaa (LV), Ida-Virumaa (IV) and Jõgevamaa (Jõ) counties; SW (South-  
678West) includes Pärnumaa (Pä) and Viljandimaa (Vi); SE (South-East) includes Valgamaa  
679(Va), Tartumaa (Ta), Põlvamaa (Põ) and Võrumaa (Võ). NA are individuals with no birth

680place information available. Individual non-Estonian samples are shown in grey. Medians of  
681non-Estonian populations are coloured according to geographic regions as shown in the  
682legend. Russians (N) and Russians (C/S) refers to Russians North and Central/South (Table  
683SI2:1.2-I). Inset in bottom left corner shows a map of Estonian counties. This map was  
684created in R (<https://www.R-project.org/>)<sup>44</sup> using an shp object of the Administrative and  
685settlement units provided by the Estonian Land Board, 2018.11.01  
686(<https://geoportaal.maaamet.ee/eng/Spatial-Data/Administrative-and-Settlement-Division->  
687p312.html). See Methods for more details.

688Figure 2. Genetic clustering of R50+ samples based on pairwise sharing of IBD segments. a,  
689Hierarchical relationships (tree) and the average total length of IBD segments shared  
690between cluster members (heatmap) as inferred by fineSTRUCTURE. The length of the tree  
691branches does not reflect any relationship between the clusters. Clusters are named to  
692reflect their geographic distribution (E - “East”, NW - “North-West”, NE - “North-East”, SW -  
693“South-West”, SE - “South-East”). Numbers in grey next to cluster names refer to the sample  
694size of each cluster. b, Geographic distribution of inferred genetic clusters. Each symbol on  
695the Estonian map corresponds to one individual from the R50+ subset. See SI1:2.3 for  
696details. This map was created in R (<https://www.R-project.org/>)<sup>44</sup> using an shp object of the  
697Administrative and settlement units provided by the Estonian Land Board, 2018.11.01  
698(<https://geoportaal.maaamet.ee/eng/Spatial-Data/Administrative-and-Settlement-Division->  
699p312.html). See Methods for more details.

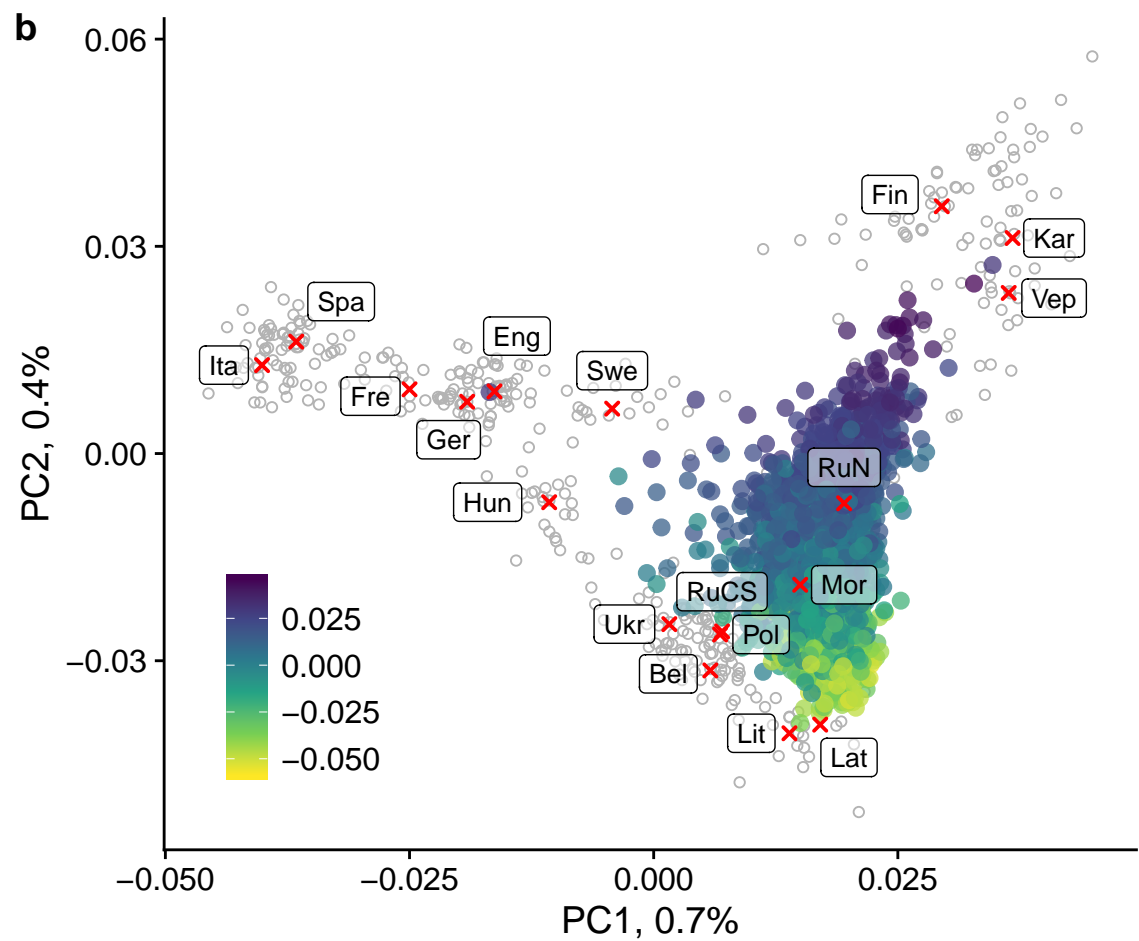
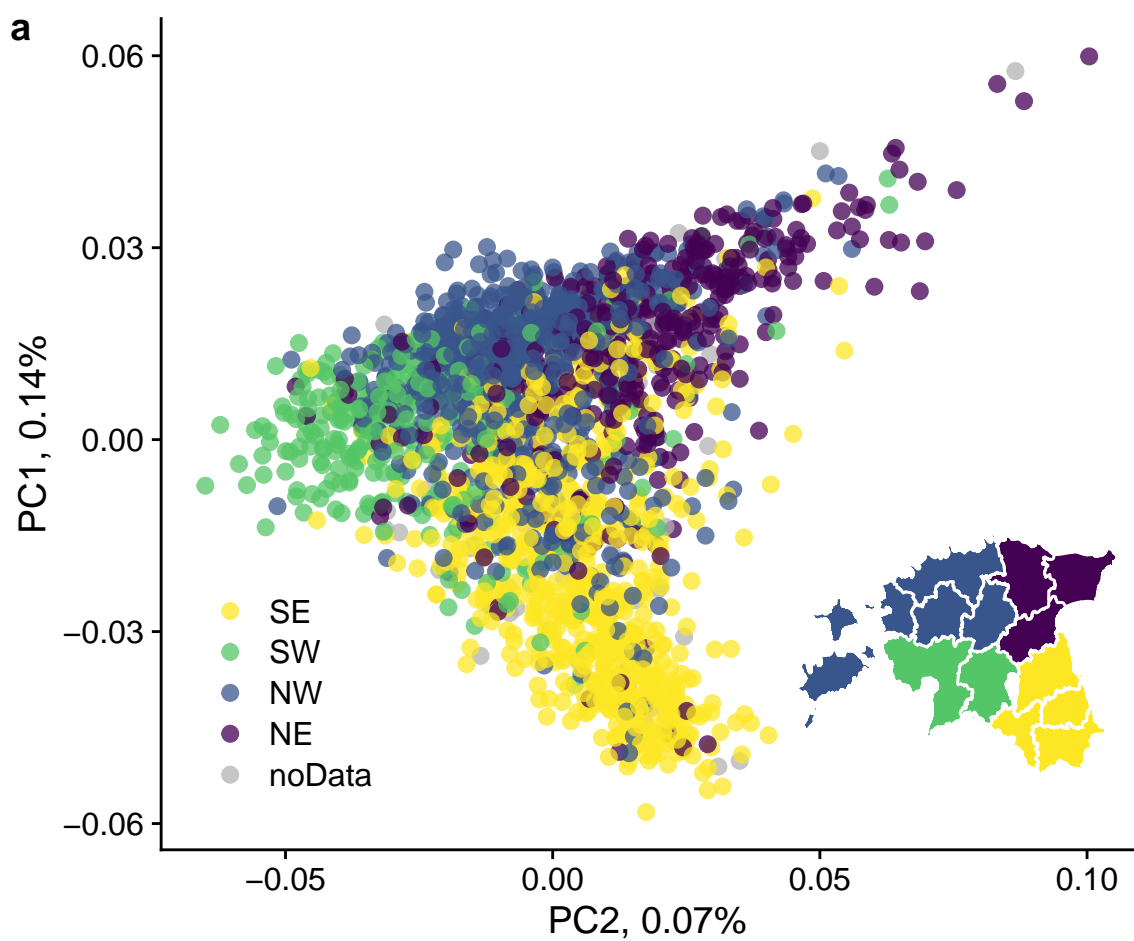
700Figure 3. Homozygosity-by-descent in the R50+ dataset. Boxplots show distribution of per-  
701genome total length of Homozygosity-By-Descent (HBD) tracts within clusters shown in  
702Figure 2. HBD tracts were detected using IBDseq13. The boxes show 25th, 50th and 75th  
703quantiles, while the whiskers show values within 1.5 times the inter-quantile range (IQR) of  
70425th and 75th quantiles. Individual dots show outliers (values out of the range shown by the  
705whiskers).

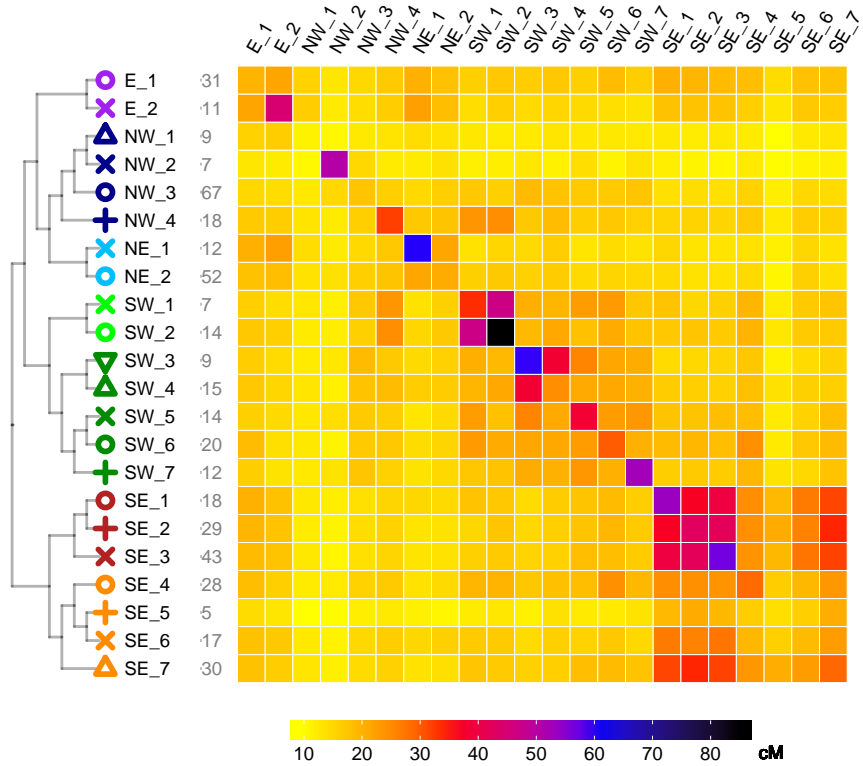
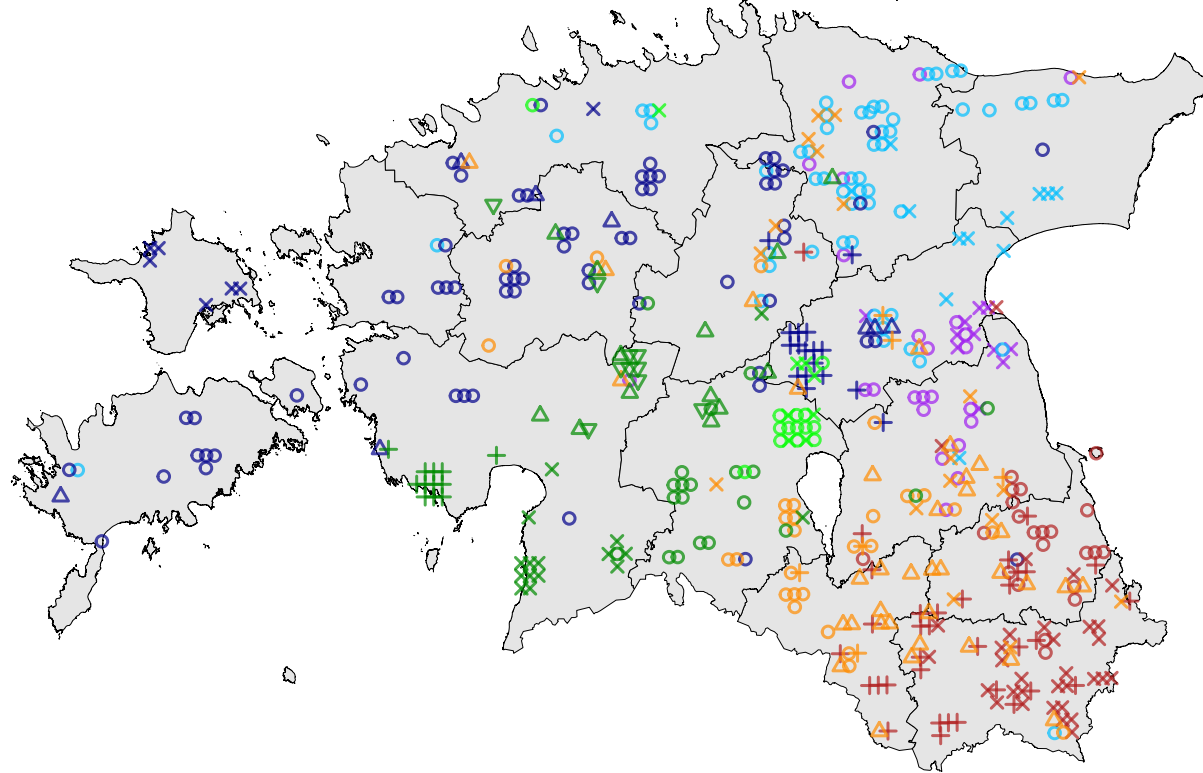
706 Figure 4. Relative proportions of “Baltic”, “Slavic”, Finnish and Swedish ancestry in the R50+  
707 subset. Modelled relative ancestral proportions of «Balts» (Latvians and Lithuanians) (a),  
708 «Slavs» (Belarusians, Poles, Russians, Ukrainians) (b), Finns (c), and Swedes (d) attributed  
709 by applying non-negative least squares approach (NNLS) to  
710 CHROMOPAINTER/fineSTRUCTURE (CP/FS) results are shown. For details on source  
711 group composition, as well as for results for other groups see SI1:3.1. The colour of each  
712 parish reflects mean values of samples coming from this parish. Parishes with no samples in  
713 the R50+ dataset are filled with grey. The scale is the same for all four panels. See SI1:3.1  
714 for more details. These maps were created in R (<https://www.R-project.org/>)<sup>44</sup> using an shp  
715 object of the Administrative and settlement units provided by the Estonian Land Board,  
716 2018.11.01 ([https://geoportaal.maaamet.ee/eng/Spatial-Data/Administrative-and-Settlement-](https://geoportaal.maaamet.ee/eng/Spatial-Data/Administrative-and-Settlement-Division-p312.html)  
717 [Division-p312.html](https://geoportaal.maaamet.ee/eng/Spatial-Data/Administrative-and-Settlement-Division-p312.html)). See Methods for more details.

718 Figure 5. Genetic clustering of the entire Estonian dataset (2,305 samples). Samples were  
719 clustered using the fineSTRUCTURE clustering algorithm based on pairwise total genetic  
720 length of IBD segments as described in Methods. Obtained clusters were pulled together  
721 based on their position on the tree resulting in 12 higher order clusters shown here (SI1:2.3).  
722 A: Hierarchical relationships (tree) and average total length of IBD segments shared  
723 between clusters (heatmap). The length of the tree branches does not reflect any  
724 relationship between the clusters. Numbers in grey next to cluster names show the number  
725 of samples in each cluster. B: Geography of inferred clusters. Each dot within the contour of  
726 Estonia corresponds to one individual, while waffle plots show samples for 15 major  
727 Estonian towns with each dot corresponding to 5 individuals. This map was created in R  
728 (<https://www.R-project.org/>)<sup>44</sup> using an shp object of the Administrative and settlement units  
729 provided by the Estonian Land Board, 2018.11.01  
730 ([https://geoportaal.maaamet.ee/eng/Spatial-Data/Administrative-and-Settlement-Division-](https://geoportaal.maaamet.ee/eng/Spatial-Data/Administrative-and-Settlement-Division-p312.html)  
731 [p312.html](https://geoportaal.maaamet.ee/eng/Spatial-Data/Administrative-and-Settlement-Division-p312.html)). See Methods for more details.

732 Figure 6. Estonian effective population size dynamics. a, Effective population size estimates  
733 obtained by applying IBDNe19 to the entire dataset and to 4 clusters from Figure 5: eNW\_1,  
734 eNE, eSW\_2 and eSE\_5. b, Comparison of historical and genetic estimates of Estonian  
735 population size. Historical estimates combine census data and reconstructions based on  
736 written or archaeological sources (S1:4.2-II). Genetic estimates are derived from IBDNe  
737 results, for which Est1527 subset was used (SI1:4.4-II) and refer to the broader population  
738 that contributed over time to the genomes of contemporary Estonians. When converting time  
739 points of the IBDNe curve into actual years we used the same logic as in the original  
740 publication19 and set generation 0 to correspond to the year when individuals in our sample  
741 had a mean age of 25 (1988). Generation time of 29 years was assumed. For year 1200 the  
742 minimum and maximum estimates are provided. In panel a shaded areas show 95%  
743 confidence intervals. In panel b shaded area corresponds to the range between the  
744 minimum and maximum genetic estimates of  $N_c$  (Methods), while the light blue line shows  
745 the geometric mean between the two. In both panels on the y axis, “k” stands for  
746 “thousands” and “M” for millions.

747 Figure 7. Genome-wide plots of positive standardized SDS scores for the entire dataset (a)  
748 as well as SE (b) and nonSE (c) subsets. Conditional suggestive (blue) and genome-wide  
749 (red) significance lines are drawn. Gene names are highlighted for intragenic variants with –  
750  $\log_{10}(p) > 5$ . Datasets are described in the text and Supplementary Information SI1:5.1.

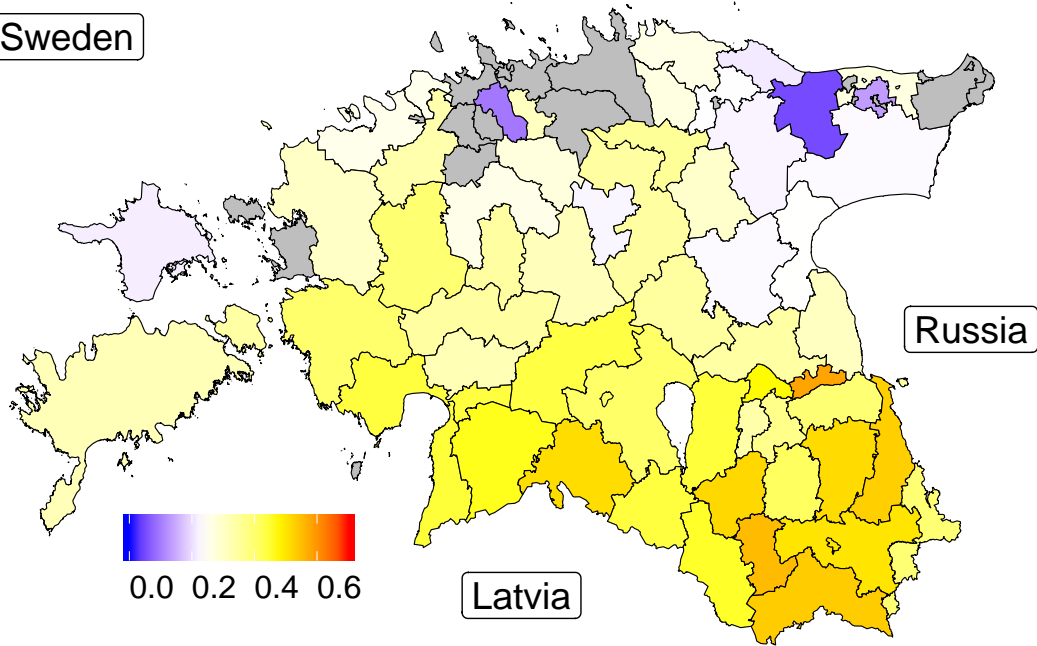


**a****b**

# Balts

Finland

Sweden



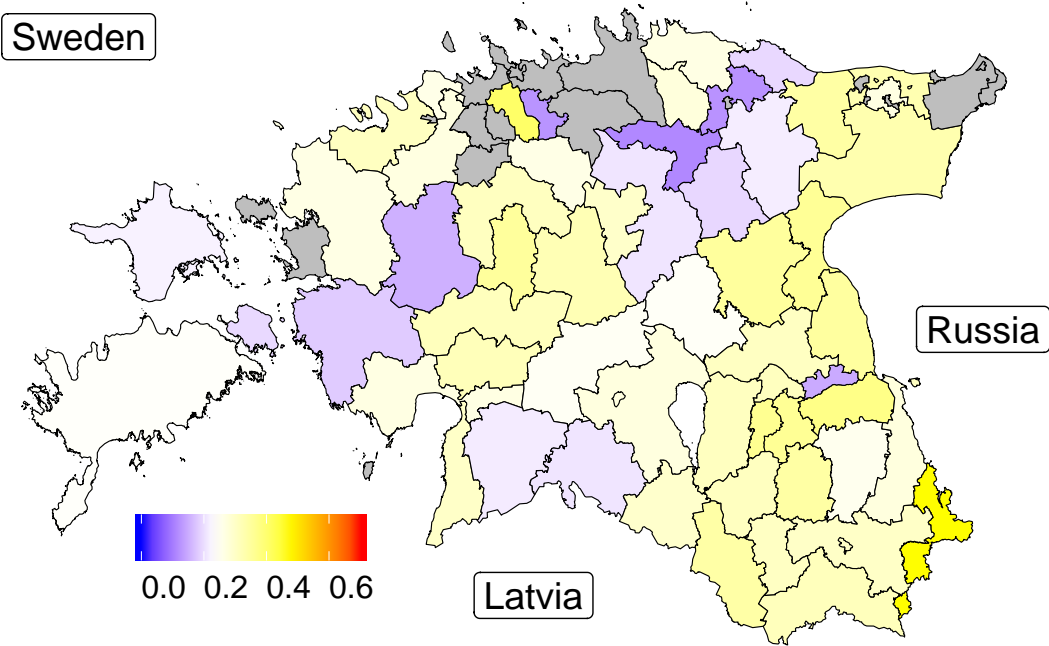
Russia

Latvia

# Slavs

Finland

Sweden



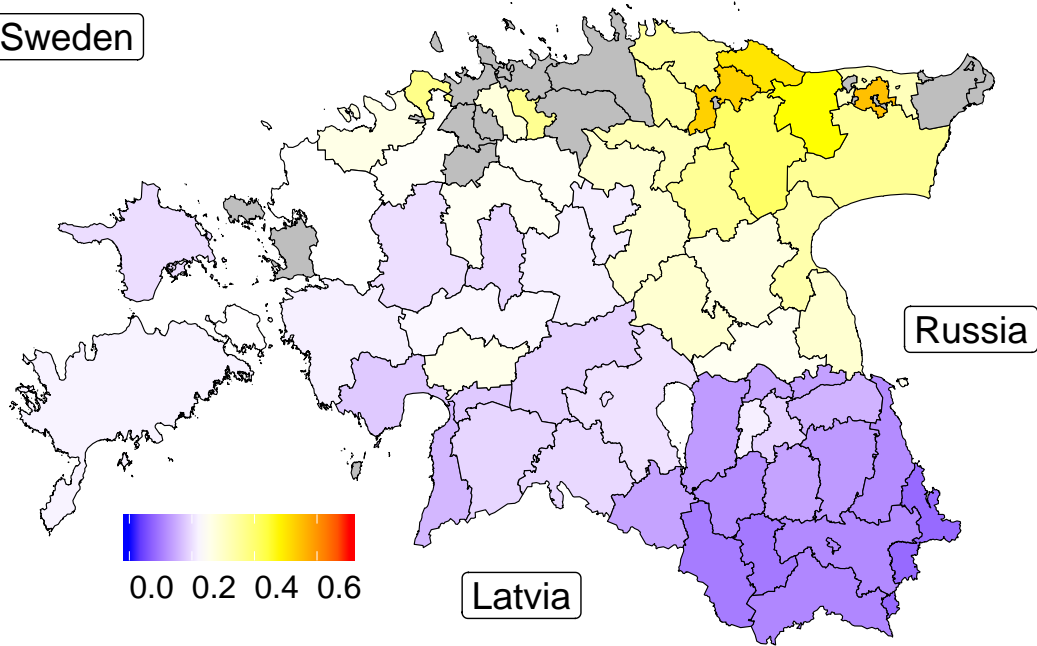
Russia

Latvia

# Finns

Finland

Sweden



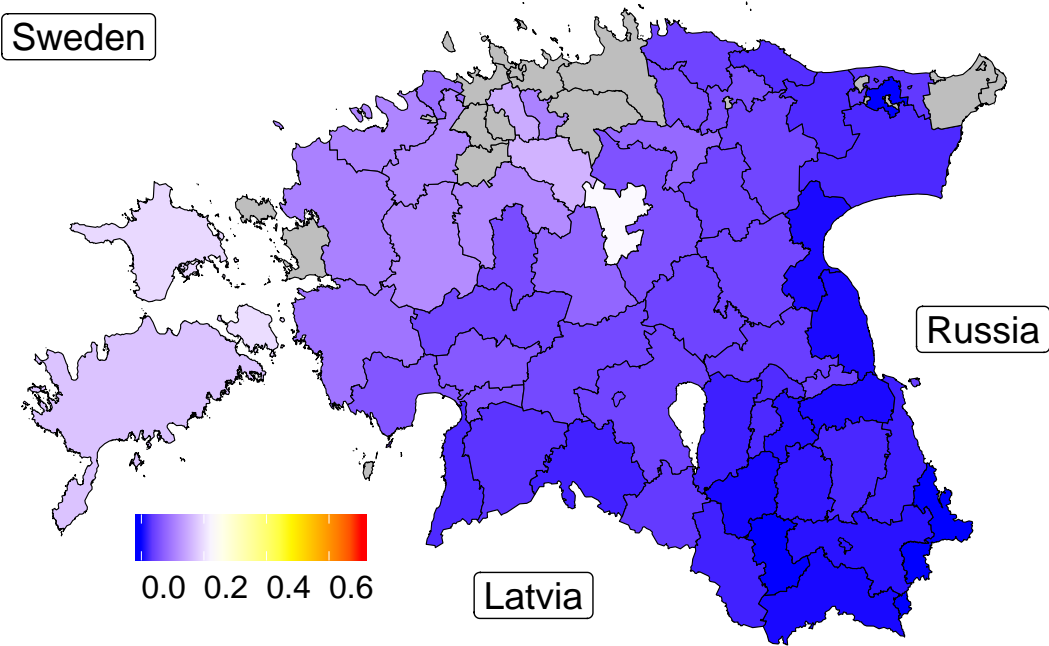
Russia

Latvia

# Swedes

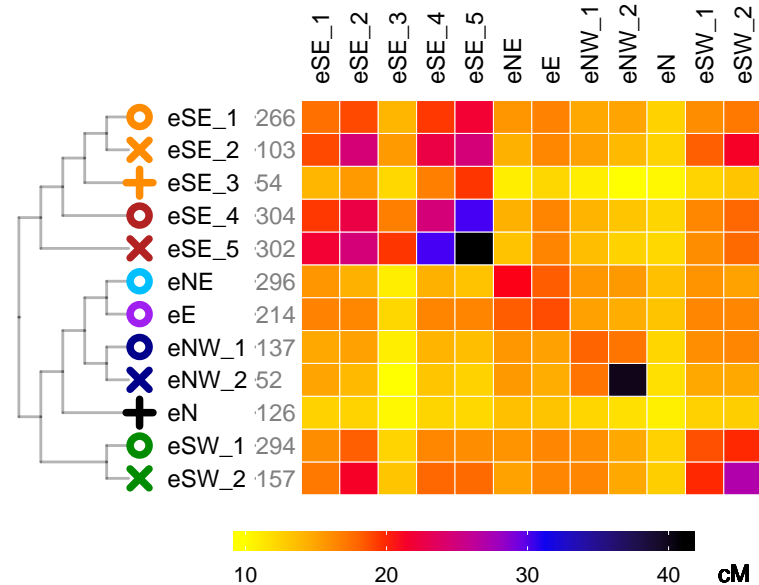
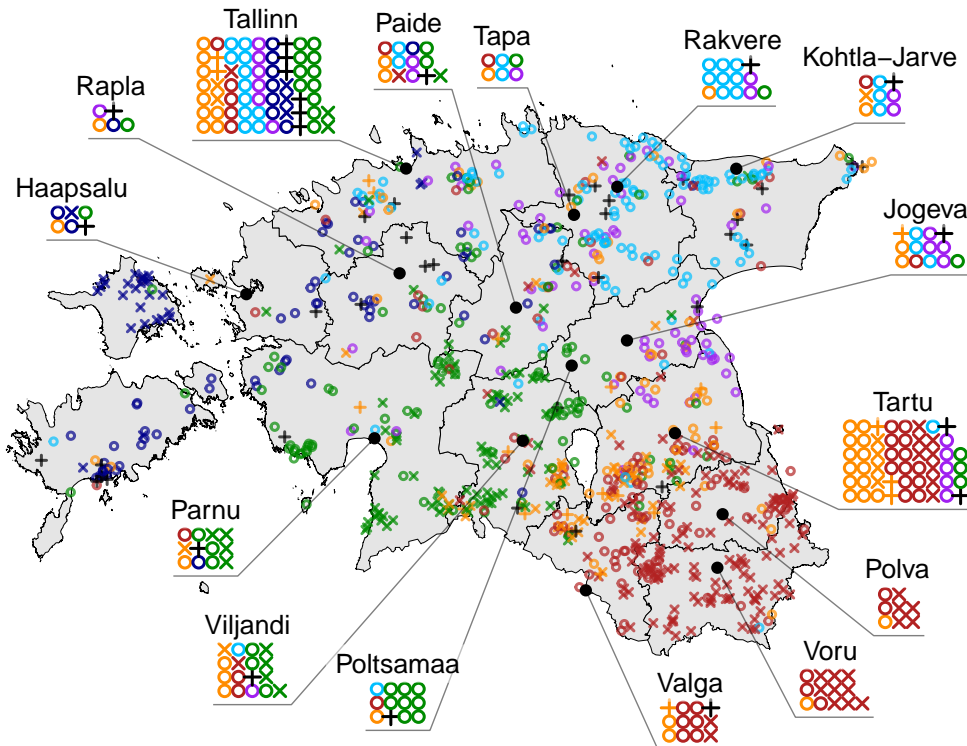
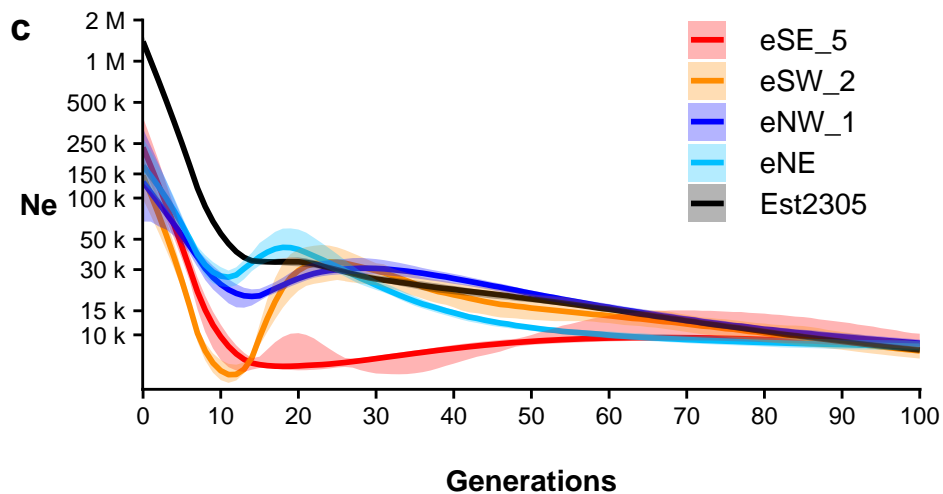
Finland

Sweden



Russia

Latvia

**a****b****c****d**